384

A reduced rank estimate of forecast error variance changes due to intermittent modifications of the observing network

Martin Leutbecher*

Research Department

* Centre National de Recherches Météorologique, Météo-France and ECMWF

Abstract

A new tool for planning adaptive observations is introduced. Different modifications of the observing network can be compared prior to the time when the modification takes place. The method predicts the variance of forecast errors projected into a low-dimensional subspace. Tangent-linear error evolution is assumed and the contribution of model errors to the forecast error is neglected. Singular vectors of the propagator of the tangent-linear version of the forecast model are used to define a relevant subspace. The method employs the Hessian of the cost function of a variational assimilation scheme to obtain information on the distribution of initial errors. Thus, this technique for planning adaptive observations can be made consistent with operational variational assimilation schemes. The application of the method is currently limited to intermittent modifications of the observing network as changes of the background error distribution due to modifications of the network in previous assimilation cycles are not accounted for. The predicted changes of forecast error variance are identical to those that the ensemble transform Kalman filter method would yield if applied to a set of Hessian singular vectors.

The reduced rank estimate has been implemented in the Integrated Forecasting System of the European Centre for Medium-Range Weather Forecasts. To illustrate the scope of the method, it is applied to the 2-day forecast of an extra-tropical cyclone. The expected reduction of the total energy of forecast error is computed for various hypothetical adaptive networks that differ by spatial coverage, observation density and the type of observation.

1   Introduction

Adaptive observations have been proposed to reduce the risk of large forecast errors. Even in the short range of 1–3 days initial errors can evolve into large forecast errors on the synoptic scale. One can hope to improve the forecast for a certain region and forecast range by taking additional observations in those places where the forecast is particularly sensitive to errors in the initial condition. Ideally, one would like to determine the optimal sites for the supplementary observations and additionally obtain an estimate of the expected reduction of the magnitude of forecast error due to the use of the additional observations. Only with such an estimate it is actually possible to define the meaning of 'optimal' sites for supplementary observations (Berliner *et al.* 1999). In principle, changes of the forecast error covariance matrix due to modifications of the observing network could be evaluated with an extended Kalman filter. However, this is computationally not feasible as the dimension of the state space of realistic NWP models is too large.

The ensemble transform method (Bishop and Toth 1999) and the ensemble transform Kalman filter method (Bishop *et al.* 2001) obtain approximations of the forecast error covariance matrices associated with modifications of the observing network. Both methods analyze the perturbations of the members of an ensemble forecast about the ensemble mean or an unperturbed control forecast assuming that the evolution of these perturbations is essentially linear. In the ensemble transform method, a guessed diagonal matrix represents the analysis error covariance matrix associated with a modification of the observing network. The guess matrix has smaller variance in the vicinity of the sites where the supplementary observations are taken. In the ensemble transform Kalman filter (ETKF) method, the analysis error covariance matrix for the modified network is consistent with the statistics of an ETKF assimilation scheme. The current operational version predicts forecast error variance reductions that deviate substantially from the actual average reductions of the magnitude of the forecast error (Majumdar *et al.* 2001). While recent research (C. Bishop, personal communication) shows that the error of the ETKF forecast error variance prediction is significantly reduced by improving the technique's routine analysis error covariance estimate, the skill of the ETKF is limited by small ensemble sizes and the inconsistency between the covariance estimates of the ETKF and the operational assimilation scheme.

Recently, Bergot and Doerenbecher (2002) have proposed a technique for planning adaptive observations that uses analysis error covariances consistent with the error estimates of an operational variational data assimilation

scheme. They consider the variance of a forecast aspect that is due to a distribution of initial errors; the reduction of this variance resulting from an observing network upgrade is computed. The variance is calculated by evaluating the analysis error covariance estimate in the direction of the sensitivity of the forecast aspect to the initial conditions. Therefore, they call this technique *Kalman filter sensitivity*. For the adaptive observing problem, the goal is to identify a set of supplementary observations that minimizes this variance. The Kalman filter sensitivity is related but not identical to the recently proposed sensitivity with respect to observations (Baker and Daley 2000; Doerenbecher and Bergot 2001). The sensitivity with respect to observations and the Kalman filter sensitivity are the only techniques so far that take the properties of an operational assimilation scheme into account.

Here, a new technique will be described to evaluate the variance of forecast error projected in a n-dimensional subspace. A norm, such as total energy, has to be chosen to normalize the variances. The variance measure can be interpreted as the expected value of the square norm of the projected forecast error due to a distribution of initial errors evolved tangent-linearly. Like the Kalman filter sensitivity, the method uses estimates of the analysis error covariances that are consistent with the statistical assumptions of a variational data assimilation scheme. In order to reduce the rank of the problem, forecast errors are projected on a subspace spanned by the leading Hessian singular vectors (Barkmeijer *et al.* 1998, Palmer *et al.* 1998). They evolve into the leading eigenvectors of the forecast error covariance matrix — assuming tangent-linear dynamics, no model error as well as covariance estimates for background error and observation error that agree with the true covariances. It is suggested to call this method the Hessian Reduced Rank estimate (HRR). The Hessian of the cost function of the variational assimilation scheme enters at two stages. First, singular vectors are computed with the Hessian metric for the routine observing network to define the n-dimensional subspace. Second, the Hessian metric for the modified observing network is computed in the subspace. In the limit, where the subspace dimension n approaches the dimension of the state space of the model N, the HRR estimate converges towards the estimate that an extended Kalman filter would give, which had been initialized with the background error covariance matrix used in the variational assimilation scheme. However, the potential advantage of the HRR estimate is the application with a subspace dimension $n \ll N$, but n being still sufficiently large to capture a relevant part of the forecast error variance.

The outline of the paper is as follows. In section 2, the methodology of the HRR is described. In section 3, the HRR is applied to a case of an extratropical cyclone; several different upgrades of the routine observing network are compared. Discussion and conclusions follow in sections 4 and 5, respectively. The appendices contain details about the projections and the approximation of the analysis error covariance matrix.

2 The Hessian reduced rank estimate

At the beginning of this section, the subspace and the projections required for the definition of the reduced rank estimate are introduced. The subspace is spanned by the Hessian singular vectors associated with the routine observing network. Next, the change of the analysis error covariance metric resulting from the modification of the observing network is considered. An eigenvalue problem restricted to the subspace is formulated using the modified metric. Its solution are a set of new vectors that are linear combinations of the routine Hessian singular vectors. The new vectors will be referred to as *subspace singular vectors* computed with the modified Hessian metric. The relation to the usual singular vectors obtained for the modified Hessian metric will be discussed in section 4. Then, it is shown that the difference between the eigenvalue spectra of the routine Hessian singular vectors and the subspace singular vectors yields an approximation for the expected change of the magnitude of the projected forecast error. The implementation of the HRR in a variational assimilation framework is discussed next. Then, it is shown that the HRR yields the same forecast error variance changes as the ensemble transform Kalman filter technique if the latter is applied to a set of Hessian singular vectors. In the last part

of this section, an alternative approximation for the analysis error covariances associated with the modified observing network is presented. With the latter approximation, the HRR estimate appears as straightforward generalization of the Kalman filter sensitivity.

2.1 Subspace and projections

Let $\mathcal{L}$ denote the N-dimensional state space of the tangent-linear version of the forecast model and $\mathbf{M}$ its propagator from the initial time t_0 to a forecast verification time t_1. Further, let $\mathbf{P}$ denote the projection operator onto the verification region. We assume that forecast errors are quantified with a norm $\| \ \|_E$ that derives from an inner product induced by the symmetric matrix $\mathbf{E}$. In the application, this will be the total energy metric but other choices for $\mathbf{E}$ may be considered also. Let $\mathbf{A}$ denote the estimate of the analysis error covariance matrix associated with the routine observing network. It is assumed that $\mathbf{A}$ has full rank. For the HRR estimate, the n-dimensional subspace $L_n \subset \mathcal{L}$ that is spanned by the leading eigenvectors $\mathbf{v}_1, \ldots, \mathbf{v}_n$ solving the following generalized eigenproblem

$$\mathbf{M}^{\mathrm{T}}\mathbf{P}^{\mathrm{T}}\mathbf{E}\mathbf{P}\mathbf{M}\mathbf{v}_i = \sigma_i^2 \mathbf{A}^{-1}\mathbf{v}_i \tag{1}$$

is selected. These vectors $\mathbf{v}_i$ are known as Hessian singular vectors for the case where $\mathbf{A}^{-1}$ is obtained from the Hessian of the cost function of a variational assimilation scheme (Barkmeijer *et al.* 1998). The subspace L_n is well suited for the reduced rank estimate as the evolved subspace $\mathbf{M}L_n$ is the n-dimensional subspace in $\mathcal{L}$ that explains most of the forecast error variance under the previously mentioned assumptions. The leading Hessian singular vectors yield the dominating part of the complete singular value decomposition of the projected propagator

$$\mathbf{P}\mathbf{M} = \mathbf{U}\boldsymbol{\Sigma}\mathbf{V}^{\mathrm{T}}\mathbf{A}^{-1}. \tag{2}$$

Here, the $N \times N$ matrix $\mathbf{V} = (\mathbf{v}_1 \ldots \mathbf{v}_N)$ contains the initial time singular vectors as columns. The matrix $\boldsymbol{\Sigma} = \mathrm{diag}(\sigma_1, \ldots, \sigma_N)$ holds the monotonically decreasing singular values $\sigma_1 \geq \sigma_2 \geq \ldots \geq \sigma_N \geq 0$. Let r denote the rank of $\boldsymbol{\Sigma}$; then $\sigma_i > 0$ for all $i \leq r$. The $N \times N$ matrix $\mathbf{U} = (\mathbf{u}_1 \ldots \mathbf{u}_N)$ contains the final time singular vectors as columns. For $i \leq r$, these are obtained from the evolved and normalized singular vectors $\mathbf{u}_i' \equiv \sigma_i^{-1}\mathbf{M}\mathbf{v}_i$ via the projection $\mathbf{u}_i = \mathbf{P}\mathbf{u}_i'$. For $i > r$, the $\mathbf{u}_i$ are an arbitrary $\mathbf{E}$-orthonormal basis in the $\mathbf{E}$-orthogonal complement of $\mathbf{P}\mathbf{M}\mathcal{L}$. The singular vectors satisfy the orthonormality relations

$$\mathbf{V}^{\mathrm{T}}\mathbf{A}^{-1}\mathbf{V} = \mathbf{I}_N \quad \text{and} \tag{3}$$

$$\mathbf{U}^{\mathrm{T}}\mathbf{E}\mathbf{U} = \mathbf{I}_N, \tag{4}$$

where $\mathbf{I}_N$ denotes the $N \times N$ identity matrix. [Note, that (2) is equivalent to the singular value decomposition $\mathbf{E}^{1/2}\mathbf{P}\mathbf{M}\mathbf{A}^{1/2} = (\mathbf{E}^{1/2}\mathbf{U})\boldsymbol{\Sigma}(\mathbf{A}^{-1/2}\mathbf{V})^{\mathrm{T}}$, in which the non-dimensionalized singular vectors $(\mathbf{A}^{-1/2}\mathbf{V})$ and $(\mathbf{E}^{1/2}\mathbf{U})$ are orthonormal in the Euclidean metric. This version of writing the singular value decomposition is consistent with the definition found in linear algebra textbooks.] The complete decomposition (2) will be used in the derivation of the HRR but only the leading n singular vectors need to be known in the application of the HRR.

The definition of projections on the initial and evolved subspaces requires the use of the same inner products as for the singular vectors. By choosing $\mathbf{A}^{-1}$ at initial time and $\mathbf{E}$ at final time, it is ensured that it does not matter whether initial errors are projected into L_n or evolved errors are projected into $\mathbf{P}\mathbf{M}L_n$. Let $\boldsymbol{\Pi}_n$ denote the $\mathbf{A}^{-1}$-orthogonal projection into the initial subspace L_n. The projection is given by

$$\boldsymbol{\Pi}_n = \mathbf{V}_n\mathbf{V}_n^{\mathrm{T}}\mathbf{A}^{-1}, \tag{5}$$

where $\mathbf{V}_n$ is the $N \times n$ matrix $(\mathbf{v}_1 \ldots \mathbf{v}_n)$. Furthermore, let $\widehat{\mathbf{\Pi}}_n$ denote the $\mathbf{E}$-orthogonal projection on the evolved and projected subspace $\mathbf{PM}L_n$. This projection is given by

$$\widehat{\mathbf{\Pi}}_n = \mathbf{U}_n \mathbf{U}_n^{\mathrm{T}} \mathbf{E}, \tag{6}$$

where $\mathbf{U}_n \equiv (\mathbf{u}_1 \ldots \mathbf{u}_n)$. Then, the projection with $\widehat{\mathbf{\Pi}}_n$ at final time is equivalent to the projection with $\mathbf{\Pi}_n$ at initial time via

$$\widehat{\mathbf{\Pi}}_n \mathbf{PM} = \mathbf{PM}\mathbf{\Pi}_n \tag{7}$$

as shown in appendix A. The reduced rank estimate will be defined as the expected value of the square norm of the forecast error projected with $\widehat{\mathbf{\Pi}}_n$. Due to the commutativity property (7), the expected value can be computed by neglecting initial errors in the $\mathbf{A}^{-1}$-orthogonal complement of the subspace L_n.

2.2 Modification of the analysis error covariance metric

A modification of the routine observing network results in a change of the analysis error covariance matrix. Let $\widetilde{\mathbf{A}}$ denote the estimate of the analysis error covariance matrix associated with the modified observing network. The key step of the HRR estimate is a linear transformation of the routine Hessian singular vectors into vectors $\tilde{\mathbf{v}}_1, \ldots \tilde{\mathbf{v}}_n$ in the subspace L_n that are orthonormal with respect to the modified Hessian metric $\widetilde{\mathbf{A}}^{-1}$. Let $\mathbf{\Gamma}$ denote a $n \times n$ transformation matrix

$$\widetilde{\mathbf{V}}_n \equiv (\tilde{\mathbf{v}}_1 \ldots \tilde{\mathbf{v}}_n) = \mathbf{V}_n \mathbf{\Gamma} \tag{8}$$

that satisfies

$$\mathbf{\Gamma}^{\mathrm{T}} \mathbf{V}_n^{\mathrm{T}} \widetilde{\mathbf{A}}^{-1} \mathbf{V}_n \mathbf{\Gamma} = \widetilde{\mathbf{V}}_n^{\mathrm{T}} \widetilde{\mathbf{A}}^{-1} \widetilde{\mathbf{V}}_n = \mathbf{I}_n. \tag{9}$$

As $\mathbf{C} \equiv \mathbf{V}_n^{\mathrm{T}} \widetilde{\mathbf{A}}^{-1} \mathbf{V}_n$ is symmetric, there is an orthogonal matrix $\mathbf{D}$ that transforms $\mathbf{C}$ into a diagonal matrix $\mathbf{D}^{\mathrm{T}} \mathbf{C} \mathbf{D} = \mathbf{\Theta}$. Thus, for the transformation $\mathbf{\Gamma} = \mathbf{D}\mathbf{\Theta}^{-1/2}$ equation (9) holds. The transformation matrix is only determined up to a rotation. Another transformation $\mathbf{\Gamma}' = \mathbf{\Gamma}\mathbf{T}$ satisfies (9) if and only if the matrix $\mathbf{T}$ is orthogonal. The choice of $\mathbf{T}$ does not affect the forecast error variance estimate as will be shown in the next subsection.

A particular choice for $\mathbf{\Gamma}$ arises if the transformed vectors are required to be the optimal perturbations $\mathbf{x}$ in the subspace L_n that maximize the ratio

$$\tilde{\sigma}^2 = \frac{\mathbf{x}^{\mathrm{T}} \mathbf{M}^{\mathrm{T}} \mathbf{P}^{\mathrm{T}} \mathbf{E} \mathbf{P} \mathbf{M} \mathbf{x}}{\mathbf{x}^{\mathrm{T}} \widetilde{\mathbf{A}}^{-1} \mathbf{x}}. \tag{10}$$

This particular set of transformed vectors will be referred to as *subspace singular vectors*. The leading subspace singular vector $\tilde{\mathbf{v}}_1$ is the structure in L_n that maximizes (10). The j-th subspace singular vector $\tilde{\mathbf{v}}_j$ optimizes (10) in the subspace of L_n, that is $\widetilde{\mathbf{A}}^{-1}$-orthogonal to span $\{\tilde{\mathbf{v}}_1, \ldots \tilde{\mathbf{v}}_{j-1}\}$. In order to obtain the subspace singular vectors the transformation matrix $\mathbf{\Gamma}$ has to solve the n-dimensional eigenproblem

$$\mathbf{V}_n^{\mathrm{T}} \mathbf{M}^{\mathrm{T}} \mathbf{P}^{\mathrm{T}} \mathbf{E} \mathbf{P} \mathbf{M} \mathbf{V}_n \mathbf{\Gamma} = \mathbf{V}_n^{\mathrm{T}} \widetilde{\mathbf{A}}^{-1} \mathbf{V}_n \mathbf{\Gamma} \widetilde{\mathbf{\Lambda}}, \tag{11}$$

where the diagonal matrix $\widetilde{\mathbf{\Lambda}} \equiv \mathrm{diag}(\tilde{\sigma}_1^2, \ldots, \tilde{\sigma}_n^2)$ contains the eigenvalues. This can be simplified to

$$\mathbf{\Gamma}^{\mathrm{T}} \mathbf{\Lambda} \mathbf{\Gamma} = \widetilde{\mathbf{\Lambda}} \tag{12}$$

by making use of (2), (4) and (9). An orthogonal matrix $\mathbf{T}$ can be determined such that $\mathbf{\Gamma} = \mathbf{D}\mathbf{\Theta}^{-1/2}\mathbf{T}$ satisfies both (9) and (12).

Next, it will be shown how the change of the forecast error variance is linked to the difference between the singular values σ_i of the routine Hessian singular vectors and the singular values $\tilde{\sigma}_i$ of the subspace singular vectors that are computed with the modified Hessian metric.

2.3   Reduction of forecast error variance

We measure forecast uncertainty with the expected value of the square of the E-norm of the forecast error in the verification region. The expected value of the square norm is equal to the total forecast error variance in the verification region normalized with the metric $\mathbf{E}$ according to

$$\mathcal{E}(\|\mathbf{PMx}\|_E^2) = \text{tr}\left(\mathbf{E}^{1/2}\mathbf{PM}\mathcal{E}(\mathbf{xx}^\mathrm{T})\mathbf{M}^\mathrm{T}\mathbf{P}^\mathrm{T}\mathbf{E}^{1/2}\right). \tag{13}$$

Here, $\mathcal{E}(\ )$ denotes the expectation operator with respect to a distribution of initial errors $\mathbf{x}$ and $\text{tr}(\ )$ the trace of a matrix. Equation (13) itself is computationally too expensive to evaluate for realistic NWP models. However, it is feasible to compute the variance of forecast errors projected with $\widehat{\boldsymbol{\Pi}}_n$ into the subspace spanned by the leading n routine Hessian singular vectors. Thus, the rank-n estimate is defined as

$$\varepsilon_n \equiv \mathcal{E}(\|\widehat{\boldsymbol{\Pi}}_n\mathbf{PMx}\|_E^2). \tag{14}$$

Using the commutativity relation (7), the expected value of the square norm of the projected forecast error becomes

$$\varepsilon_n = \mathcal{E}(\|\mathbf{PM}\boldsymbol{\Pi}_n\mathbf{x}\|_E^2) = \text{tr}\left(\mathbf{E}^{1/2}\mathbf{PM}\boldsymbol{\Pi}_n\mathcal{E}(\mathbf{xx}^\mathrm{T})\boldsymbol{\Pi}_n^\mathrm{T}\mathbf{M}^\mathrm{T}\mathbf{P}^\mathrm{T}\mathbf{E}^{1/2}\right). \tag{15}$$

The expectation $\mathcal{E}(\mathbf{xx}^\mathrm{T})$ is equal to the analysis error covariance matrix $\mathbf{A}$ if the routine observing network is used and to the covariance matrix $\widetilde{\mathbf{A}}$ if the modified observing network is used.

From (3), it follows that the estimate of the analysis error covariance matrix associated with the routine observing network can be represented by $\mathbf{A} = \mathbf{VV}^\mathrm{T}$. Therefore, the covariance matrix of analysis errors projected on the subspace L_n is given by

$$\boldsymbol{\Pi}_n\mathbf{A}\boldsymbol{\Pi}_n^\mathrm{T} = \mathbf{V}_n\mathbf{V}_n^\mathrm{T}\mathbf{A}^{-1}\mathbf{VV}^\mathrm{T}\mathbf{A}^{-1}\mathbf{V}_n\mathbf{V}_n^\mathrm{T} = \mathbf{V}_n\mathbf{V}_n^\mathrm{T}. \tag{16}$$

With (16), the reduced rank estimate of forecast error variance becomes

$$\varepsilon_n = \text{tr}(\mathbf{E}^{1/2}\mathbf{PMV}_n\mathbf{V}_n^\mathrm{T}\mathbf{M}^\mathrm{T}\mathbf{P}^\mathrm{T}\mathbf{E}^{1/2}) = \text{tr}(\mathbf{V}_n^\mathrm{T}\mathbf{M}^\mathrm{T}\mathbf{P}^\mathrm{T}\mathbf{EPMV}_n) = \text{tr}(\boldsymbol{\Lambda}) = \sum_{i=1}^n \sigma_i^2. \tag{17}$$

For the modified observing network, the representation of the covariance matrix of projected analysis errors is slightly more complex as the inner product used for the projection is not based on the modified metric $\widetilde{\mathbf{A}}^{-1}$ but the routine metric $\mathbf{A}^{-1}$. The projection on the subspace of routine Hessian singular vectors needs to be orthogonal with respect to the routine metric in order to ensure the commutativity property (7). In order to find an approximate representation of $\boldsymbol{\Pi}_n\widetilde{\mathbf{A}}\boldsymbol{\Pi}_n^\mathrm{T}$ we proceed as follows. First, the vectors $\tilde{\mathbf{v}}_1,\ldots,\tilde{\mathbf{v}}_n \in L_n$ are extended with vectors $\tilde{\mathbf{v}}_{n+1},\ldots,\tilde{\mathbf{v}}_N \in L_n^\perp$, the $\mathbf{A}^{-1}$-orthogonal complement of L_n, to a basis of $\mathcal{L}$, such that

$$\tilde{\mathbf{v}}_i^\mathrm{T}\widetilde{\mathbf{A}}^{-1}\tilde{\mathbf{v}}_j = \delta_{ij} \text{ for all } i,j \in \{n+1,\ldots,N\}. \tag{18}$$

This assumes that $\widetilde{\mathbf{A}}^{-1}$ has full rank. Let $\widetilde{\mathbf{V}} = (\tilde{\mathbf{v}}_1 \ldots \tilde{\mathbf{v}}_N)$ denote the matrix of column vectors of the entire basis. Vectors in $L_n^\perp$ are not necessarily $\widetilde{\mathbf{A}}^{-1}$-orthogonal to vectors in L_n. Therefore, the modified metric expressed in the basis $\widetilde{\mathbf{V}}$ is

$$\widetilde{\mathbf{V}}^\mathrm{T}\widetilde{\mathbf{A}}^{-1}\widetilde{\mathbf{V}} = \begin{pmatrix} \mathbf{I}_n & \mathbf{F} \\ \mathbf{F}^\mathrm{T} & \mathbf{I}_{N-n} \end{pmatrix}, \tag{19}$$

where $\mathbf{F}$ represents an unknown $n \times (N-n)$ matrix. Inverting (19) yields

$$\widetilde{\mathbf{A}} = \widetilde{\mathbf{V}} \begin{pmatrix} (\mathbf{I}_n - \mathbf{FF}^\mathrm{T})^{-1} & -(\mathbf{I}_n - \mathbf{FF}^\mathrm{T})^{-1}\mathbf{F} \\ -\mathbf{F}^\mathrm{T}(\mathbf{I}_n - \mathbf{FF}^\mathrm{T})^{-1} & \mathbf{I}_{N-n} + \mathbf{F}^\mathrm{T}(\mathbf{I}_n - \mathbf{FF}^\mathrm{T})^{-1}\mathbf{F} \end{pmatrix} \widetilde{\mathbf{V}}^\mathrm{T}. \tag{20}$$

Now, the covariance matrix of projected analysis errors can be written as

$$\mathbf{\Pi}_n \widetilde{\mathbf{A}} \mathbf{\Pi}_n^{\mathrm{T}} = \widetilde{\mathbf{V}}_n (\mathbf{I}_n - \mathbf{F}\mathbf{F}^{\mathrm{T}})^{-1} \widetilde{\mathbf{V}}_n^{\mathrm{T}}. \tag{21}$$

If the modification of the observing network is not too drastic, vectors in $L_n^{\perp}$ should remain nearly $\widetilde{\mathbf{A}}^{-1}$-orthogonal to vectors in L_n. Thus, the quadratic term in $\mathbf{F}$ will be a small perturbation of the identity matrix $\mathbf{I}_n$ in (21). An obvious approximation in this context is to neglect the contribution from $\mathbf{F}$ to the projected covariance matrix by using

$$\mathbf{\Pi}_n \widetilde{\mathbf{A}} \mathbf{\Pi}_n^{\mathrm{T}} \approx \widetilde{\mathbf{V}}_n \widetilde{\mathbf{V}}_n^{\mathrm{T}}. \tag{22}$$

In appendix B, an improved approximation of (21) is introduced that uses a truncated $\mathbf{F}$ computed in a higher-dimensional subspace $L_{n'} \supset L_n$. This improved approximation is then used to assess the less accurate approximation (22). The comparison indicates, that the estimate of forecast error variance based on the cruder approximation (22) is already quite accurate for subspace dimension $n > 5$. Only for lower dimensional subspaces the use of the improved approximation seems to be required. Before proceeding further, we observe that the covariance matrix $\widetilde{\mathbf{V}}_n \widetilde{\mathbf{V}}_n^{\mathrm{T}}$ would arise without approximation if the projection $\mathbf{\Pi}_n$ was replaced by the $\widetilde{\mathbf{A}}^{-1}$-orthogonal projection on the subspace L_n of routine Hessian singular vectors. However, the latter projection violates the commutativity property (7).

With (22), the reduced rank estimate of forecast error variance is approximated by

$$\tilde{\varepsilon}_n \approx \mathrm{tr}(\mathbf{E}^{1/2} \mathbf{P} \mathbf{M} \widetilde{\mathbf{V}}_n \widetilde{\mathbf{V}}_n^{\mathrm{T}} \mathbf{M}^{\mathrm{T}} \mathbf{P}^{\mathrm{T}} \mathbf{E}^{1/2}) = \mathrm{tr}(\mathbf{\Gamma}^{\mathrm{T}} \mathbf{\Lambda} \mathbf{\Gamma}) \tag{23}$$

for the modified observing network. The estimate of forecast error variance is invariant if the transformation $\mathbf{\Gamma}$ is replaced by $\mathbf{\Gamma T}$, with an orthogonal matrix $\mathbf{T}$. If $\mathbf{\Gamma}$ is chosen so that the transformed vectors are the subspace singular vectors, the forecast error variance is given by their singular values

$$\mathrm{tr}(\mathbf{\Gamma}^{\mathrm{T}} \mathbf{\Lambda} \mathbf{\Gamma}) = \mathrm{tr}(\widetilde{\mathbf{\Lambda}}) = \sum_{i=1}^{n} \tilde{\sigma}_i^2. \tag{24}$$

The difference $r_n \equiv \varepsilon_n - \tilde{\varepsilon}_n$ is the expected value of the change of the square norm of the projected forecast error due to a modification of the observing network. Using (23) and (24) the difference is approximated by

$$r_n \approx \sum_{i=1}^{n} \sigma_i^2 - \sum_{i=1}^{n} \tilde{\sigma}_i^2. \tag{25}$$

We will refer to r_n as the *reduction of forecast error variance* for short because r_n is positive if the forecast error variance decreases due to the network modification.

2.4 Implementation

In order to compute the transformation $\mathbf{\Gamma}$ the matrix $\mathbf{C} = \mathbf{V}_n^{\mathrm{T}} \widetilde{\mathbf{A}}^{-1} \mathbf{V}_n$ is required. Its computation is described now. The HRR estimate is based on a variational assimilation framework. It is assumed that the assimilation scheme uses the incremental formulation which results in a quadratic cost function. That is the difference between analysis and first guess is obtained as that perturbation of the first guess that minimizes a quadratic cost function. As outlined in Barkmeijer *et al.* (1998) the Hessian of the cost function provides an estimate of the inverse of the analysis error covariance matrix: $\nabla\nabla J = \mathbf{A}^{-1}$ (see also Rabier and Courtier 1992). Only the routine observations are used in the cost function J to get the metric $\mathbf{A}^{-1}$ associated with the routine observing network.

The modified analysis error covariance metric $\widetilde{\mathbf{A}}^{-1}$ is obtained by computing the Hessian with a modified cost function $\tilde{J}$, which measures the departure of the trajectory from the modified observing network. Then, $\nabla\nabla\tilde{J} = \widetilde{\mathbf{A}}^{-1}$. The matrix $\mathbf{C} = \mathbf{V}_n^{\mathrm{T}}\widetilde{\mathbf{A}}^{-1}\mathbf{V}_n$ can be calculated via the two following steps. First, the action of the inverse of the analysis error covariance matrix on the basis vectors of the subspace is computed using

$$\widetilde{\mathbf{A}}^{-1}\mathbf{v}_i = \nabla\tilde{J}(\mathbf{v}_i + \mathbf{x}_0) - \nabla\tilde{J}(\mathbf{x}_0) \text{ for } i = 1,\ldots n. \tag{26}$$

The latter relation holds because the cost function is quadratic. For subspace dimension n, $n+1$ computations of the gradient of the cost function are required. Then, the $n(n+1)/2$ inner products $\mathbf{v}_j^{\mathrm{T}}(\widetilde{\mathbf{A}}^{-1}\mathbf{v}_i), i = 1,\ldots,n$ and $j = i,\ldots,n$ are computed. The additional cost of diagonalizing $\mathbf{C}$ is marginal as long as the dimension n is moderate, say less than 100. The computational cost of determining $\mathbf{C}$ this way is considerably lower than the cost of computing the subspace L_n itself.

Before proceeding further, let us consider the effect of a set of supplementary observations on the analysis error covariance metric. The modified cost function can be written as

$$\tilde{J}(\mathbf{x}) = J(\mathbf{x}) + \tfrac{1}{2}(\mathbf{d}_s - \mathbf{H}_s\mathbf{x})^{\mathrm{T}}\mathbf{R}_s^{-1}(\mathbf{d}_s - \mathbf{H}_s\mathbf{x}), \tag{27}$$

where $\mathbf{d}_s, \mathbf{H}_s$ and $\mathbf{R}_s$ denote the departure of the observed values from the background, the observation operator and the observation error covariance matrix for the supplementary observations, respectively. Taking the Hessian of (27) yields

$$\widetilde{\mathbf{A}}^{-1} = \mathbf{A}^{-1} + \mathbf{H}_s^{\mathrm{T}}\mathbf{R}_s^{-1}\mathbf{H}_s. \tag{28}$$

Note that (28) is independent of the observed values. By using (28) and the orthonormality of the routine Hessian singular vectors (3), the matrix $\mathbf{C}$ can be expressed as

$$\mathbf{C} = \mathbf{I}_n + \mathbf{V}_n^{\mathrm{T}}\mathbf{H}_s^{\mathrm{T}}\mathbf{R}_s^{-1}\mathbf{H}_s\mathbf{V}_n. \tag{29}$$

This method of determining $\mathbf{C}$ requires only the evaluation of the observation operator $\mathbf{H}_s$ for the leading n routine Hessian singular vectors $\mathbf{v}_i$. This latter approach is computationally significantly more efficient than the former approach based on the gradient of the cost function.

2.5 Relationship to the Ensemble Transform Kalman Filter

The specification of the analysis error covariances by the outer product of singular vectors is reminiscent of the formulation used in the ensemble transform methods. In the latter, the routine covariances are represented as outer product of a set of ensemble perturbations. The analysis error covariances associated with the modified observing network are written as outer product of the transformed ensemble perturbations. Formally, the approach in the HRR estimate is identical as it uses the outer product of the transformed singular vectors (22) to represent the modified covariance matrix. A difference between the two methods can be hidden in the transformation. In the ensemble transform method proposed by Bishop and Toth (1999), the transformation is consistent with a guessed diagonal analysis error covariance matrix and therefore certainly different from the transformation of the HRR, which is consistent with the analysis error covariance estimate of the variational assimilation scheme. In the ensemble transform Kalman filter method (ETKF, Bishop *et al.* 2001), a transformation is used that is consistent with the statistics of the ETKF assimilation scheme. Therefore, one would expect to obtain a different transformation. However, it will be shown now that there is an equivalence between the transformation of the HRR and the transformation of the ETKF applied to the set of routine Hessian singular vectors instead of an ensemble.

The ensemble transform Kalman filter is based on transformations of the matrix of ensemble perturbations $\mathbf{Z} = (\mathbf{z}_1 \ldots \mathbf{z}_n)$ about the ensemble mean. The perturbations $\mathbf{z}_i$, valid at the time of the network modification,

are typically obtained from an evolved ensemble and are suitably scaled so that $\mathbf{Z}\mathbf{Z}^{\mathrm{T}}$ yields a useful estimate of the analysis error covariance matrix associated with the routine observing network. Then, an augmentation of the routine observing network is considered. In the ETKF approach a $n \times n$ transformation matrix $\mathbf{\Gamma}_{\mathrm{ETKF}}$ is determined such that $\mathbf{Z}\mathbf{\Gamma}_{\mathrm{ETKF}}\mathbf{\Gamma}_{\mathrm{ETKF}}^{\mathrm{T}}\mathbf{Z}^{\mathrm{T}}$ is the analysis error covariance estimate associated with the modified observing network. This estimate assumes that the supplementary observations are assimilated with an ETKF and that the ensemble based error covariances are accurate. The transformation matrix is given by

$$\mathbf{\Gamma}_{\mathrm{ETKF}} = \mathbf{T}(\mathbf{\Phi} + \mathbf{I}_n)^{-1/2}, \tag{30}$$

where the orthogonal matrix $\mathbf{T}$ and the diagonal matrix $\mathbf{\Phi}$ solve the n-dimensional eigenproblem

$$(\mathbf{Z}^{\mathrm{T}}\mathbf{H}_s^{\mathrm{T}}\mathbf{R}_s^{-1}\mathbf{H}_s\mathbf{Z})\mathbf{T} = \mathbf{T}\mathbf{\Phi}. \tag{31}$$

Here, $\mathbf{H}_s$ and $\mathbf{R}_s$ denote again the observation operator and the observation error covariance matrix for the supplementary observations. Now we consider that the ensemble perturbations $\mathbf{Z}$ are replaced by the routine Hessian singular vectors $\mathbf{V}_n$ in (31). This yields a transformation $\mathbf{\Gamma}_{\mathrm{ETKF}}$ that renders the transformed vectors $\mathbf{V}_n\mathbf{\Gamma}_{\mathrm{ETKF}}$ orthonormal with respect to the modified Hessian metric $\widetilde{\mathbf{A}}^{-1}$. This follows immediately from (28) and (31).

Thus, the transformation matrices of the HRR and the ETKF applied to a set of routine Hessian singular vectors are identical up to a rotation. In consequence, the reduction of forecast error variance predicted by the ETKF applied to the routine Hessian singular vectors will be identical to the reduction predicted by the HRR if the tangent-linear model is used to evolve the singular vectors to the verification time and if the same metric is used to measure forecast errors.

2.6   An alternative approximation

An alternative method of estimating the reduction of forecast error variance can be formulated. This approach is based on a representation of the analysis error covariances following the work of Fisher and Courtier (1995). The analysis error covariance matrix for the routine observing network is approximated by a low rank correction of the assimilation scheme's estimate of the background error covariance matrix $\mathbf{B}$

$$\mathbf{A} \approx \mathbf{B} - \sum_{j=1}^{K}(1 - \lambda_j^{-1})(\mathbf{L}\mathbf{w}_j)(\mathbf{L}\mathbf{w}_j)^{\mathrm{T}}. \tag{32}$$

The correction uses the leading eigenpairs $(\lambda_j, \mathbf{w}_j)$ of the Hessian of the cost function for the routine observing network. The eigenpairs can be determined approximately with a combined Lanczos/conjugate gradient method during the minimization of the cost function. The eigenpairs are computed in control space; that is the space in which the background error covariance matrix is the identity. The operator $\mathbf{L}$ denotes the transformation from control space to model space. In order to be consistent with (32), the forecast errors have to be projected on the subspace spanned by the leading singular vectors computed with the inverse of (32) as initial time metric. These approximate Hessian singular vectors can be computed as solution of an ordinary eigenproblem as the square root of (32) is available. This has the advantage that the computational cost is significantly lower than that of solving the generalized eigenproblem (1). To achieve consistency, the projection on the subspace also has to use the inverse of (32) as metric.

For the routine network augmented by a set of supplementary observations, the analysis error covariance matrix is represented by

$$\widetilde{\mathbf{A}} = \mathbf{A} - \mathbf{A}\mathbf{H}_s^{\mathrm{T}}\left(\mathbf{R}_s + \mathbf{H}_s\mathbf{A}\mathbf{H}_s^{\mathrm{T}}\right)^{-1}\mathbf{H}_s\mathbf{A}, \tag{33}$$

where $\mathbf{A}$ is given by (32). Operators with subscript s refer again to the supplementary observations. This relation can be derived from (28) with the Sherman-Morrison and Woodbury formula. Using (33), the projected version of $\widetilde{\mathbf{A}}$ is given by

$$\mathbf{\Pi}_n\widetilde{\mathbf{A}}\mathbf{\Pi}_n^{\mathrm{T}} = \mathbf{V}_n(\mathbf{I}_n - \mathbf{S})\mathbf{V}_n^{\mathrm{T}} \quad \text{with} \tag{34}$$

$$\mathbf{S} \equiv \mathbf{V}_n^{\mathrm{T}}\mathbf{H}_s^{\mathrm{T}}\left(\mathbf{R}_s + \mathbf{H}_s\mathbf{A}\mathbf{H}_s^{\mathrm{T}}\right)^{-1}\mathbf{H}_s\mathbf{V}_n. \tag{35}$$

With this representation of the projected covariance matrix, the variance of forecast error projected onto the subspace turns out to be $\tilde{\varepsilon}_n = \mathrm{tr}\left((\mathbf{I}_n - \mathbf{S})\mathbf{\Lambda}\right)$. Therefore, the reduction of forecast error variance is given by

$$r_n = \mathrm{tr}\left(\mathbf{S}\mathbf{\Lambda}\right). \tag{36}$$

To evaluate (35) the inverse of the matrix $\mathbf{R}_s + \mathbf{H}_s\mathbf{A}\mathbf{H}_s^{\mathrm{T}}$ is required. The matrix can be inverted directly as long as the number of supplementary observations is small enough, say less than 10^3. This limit would be reached for instance with 20 supplementary radiosondes having 50 pieces of data per sounding. Iterative techniques for the inversion seem more appropriate for larger modifications of the observing network.

Representations (32) and (33) are employed by Bergot and Doerenbecher (2002) for the Kalman filter sensitivity. It predicts the reduction in variance of a forecast aspect $\mathcal{J}$. In the tangent-linear approximation this reduction of variance is given by

$$r_{\mathcal{J}} = (\nabla_{\mathbf{x}}\mathcal{J})^{\mathrm{T}}\mathbf{A}\mathbf{H}_s^{\mathrm{T}}\left(\mathbf{R}_s + \mathbf{H}_s\mathbf{A}\mathbf{H}_s^{\mathrm{T}}\right)^{-1}\mathbf{H}_s\mathbf{A}\nabla_{\mathbf{x}}\mathcal{J}, \tag{37}$$

where $\nabla_{\mathbf{x}}\mathcal{J}$ denotes the sensitivity with respect to the initial conditions. If $\mathbf{A}\nabla_{\mathbf{x}}\mathcal{J}$ is replaced by the scaled leading singular vector $\sigma_1\mathbf{v}_1$ in (37), the rank-one estimate is obtained, cf. (35) and (36). Thus, in this approximation the Kalman filter sensitivity and the rank-one estimate are closely related. The only difference is the direction in phase space for which the change of variance is estimated. The potential advantage of the reduced rank estimate is that it can be used to assess the change of forecast error variance in many directions whereas the Kalman filter sensitivity is limited to one direction. In addition, the directions chosen for the reduced rank estimate are the leading eigenvectors of the routine forecast error covariance matrix and are thus influenced by the tangent-linear dynamics. On the contrary, the direction in phase space on which forecast errors are projected in the Kalman filter sensitivity is independent of the tangent-linear dynamics and depends only on the choice of the forecast aspect $\mathcal{J}$ and possibly the nonlinear dynamics. The latter dependence arises through the trajectory used for linearization if the forecast aspect is a nonlinear function of the state vector at verification time.

3 Application to the forecast of an extra-tropical cyclone

The HRR estimate is now applied in diagnostic mode to the case of the severe storm that crossed France and Germany on 26 December 1999. The Hessian singular vectors are computed on a trajectory starting from the analysis valid at the network modification time and the Hessian is based on the actual routine observations of this analysis cycle. The reductions of forecast error variance due to several adaptive upgrades of the observing network are compared (Table 1). The forecast error is quantified with the total energy norm localized to the region 20°W–20°E, 35°–60°N. A forecast range of 48 hours is considered with a verification time at 12 UTC on 26 December 1999. Leutbecher *et al.* (2002) discuss impact experiments for some of the configurations of adaptive observations that are considered here. Their impact experiments use synthetic observations constructed from a simulated truth. Here, the observations are also synthetic but the observed values are irrelevant apart from the quality control decisions in the assimilation scheme. The Hessian metric depends only on the observation error statistics, the distribution of observations in space-time and the background error statistics.

The forecast error variance for the modified observing network is computed via the improved approximation described in appendix B. For all subspace dimensions up to 25, the projected analysis error covariance matrix is constructed based on the Hessian in the subspace of the 25 leading routine Hessian singular vectors. The improved approximation introduces a small but noticeable correction for small subspace dimensions, say less than five.

The HRR estimate has been implemented for the Integrated Forecasting System of the European Centre for Medium-Range Weather Forecasts. As data-assimilation scheme a 6-hour 4D-Var is used. The spatial resolution of the Hessian singular vectors is T42 in the horizontal and 31 levels in the vertical. The analysis error covariance metric is evaluated at the spatial resolution of the singular vectors. Tangent-linear and adjoint versions of the forecast model are used that are adiabatic and frictionless apart from diffusion and surface drag. A climatological estimate is employed for the background error covariances. It stems from an ensemble of assimilations and forecasts in which the observed values are perturbed in order to represent observational error (Fisher and Andersson 2001).

Exp.	N_{snd}	Δs	vars.	location	r_{25}/ε_{25}
a	0	–	–	–	0.00
b	160	280	all	Pacific	0.00
c	160	280	all	target L	0.62
d	10	560	all	target M	0.16
e	10	280	all	target S	0.16
f	40	560	all	target L	0.31
g	40	280	all	target M	0.38
h	40	94	all	flight-track in target M	0.37
i	40	280	all	target M, sfc–600hPa	0.25
j	40	280	all	target M, 600–200hPa	0.21
k	40	280	wind	target M	0.28
l	40	280	temp.	target M	0.19
m	640	280	temp.	target XL	0.44
n	640	280	all	target XL	0.70
o	40	280	all	TESV target M	0.27
p	40	111	all	target XS	0.30
q	40	1110	all	target XL	0.14

Table 1: Configurations of supplementary soundings and the fractional reduction of the total energy of forecast error r_{25}/ε_{25} for subspace dimension 25. Here, N_{snd} denotes the number of soundings, Δs the spacing between the soundings in km, vars. the observed variables (all meaning wind and temperature).

3.1   Spatial distribution of supplementary observations

In this section it is investigated how the expected reduction of the total energy of the forecast error depends on the spatial distribution of supplementary observations. Soundings of wind and temperature from 200 hPa to the surface are considered as supplementary observations. The observation error of the supplementary data is characterized by the error variances used operationally for radiosondes. The goal is to identify distributions of soundings that lead to a large reduction of the variance of forecast error projected into the subspace spanned by the 25 leading routine Hessian singular vectors. The optimal region to place the supplementary observations is obviously linked to the region where these singular vectors have the largest amplitude at initial time. Therefore,

the weighted average $\eta \equiv \sum_{i=1}^{25} \sigma_i^2 \tau_i$ of the vertically integrated total energy τ_i of singular vector i is used to target the supplementary observations. The fastest growing structures are emphasized by using the squared singular values as weights. A target is defined as the region where η exceeds a threshold value. By choosing successively smaller thresholds targets of increasing size are determined. Five sizes are considered. The targets are named XS, S, M, L, XL according to their sizes 0.5, 0.8, 3, 13 and $50 \times 10^6\,\text{km}^2$. Target XL covers 10% of the earth's surface.

As a first test, the expected total energy of the forecast error of three configurations of the observing network is compared: (i) the routine network, (ii) the routine network plus 160 soundings in target L and (iii) the routine network plus 160 soundings in the Pacific — far upstream of target L (Fig. 1). With the last configuration the expected total energy of forecast error is unchanged as compared to the routine observing network. However, the upgrade with soundings in target L has a major impact. The expected total energy of forecast error is reduced to 38% of the value obtained with the routine observing network at a subspace dimension of 25. In the following plots, the reduction of forecast error variance r_n is normalized with the forecast error variance ε_n of the routine network. The quantity r_n/ε_n will be referred to as fractional reduction of forecast error variance or fractional reduction of the (expected) total energy of forecast error.
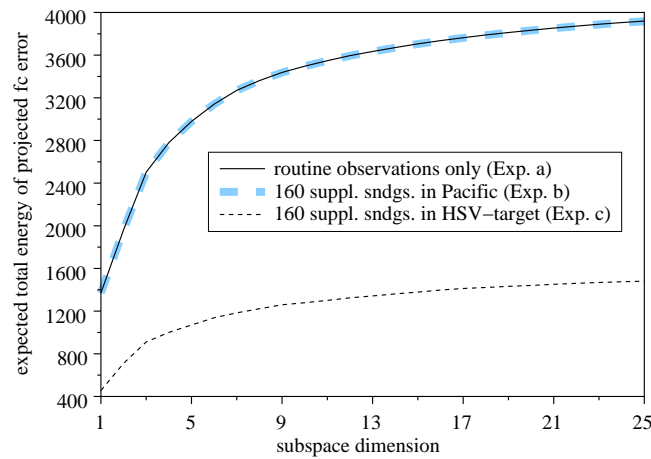

Figure 1: Expected value of total energy of projected forecast error versus subspace dimension n for three different observing networks.

The reduction of forecast error variance will increase with the number of supplementary observations. An important issue in observation targeting is to determine the appropriate size of an observing network upgrade. To illustrate this, target regions S, M, L and XL are considered. These regions are sampled with soundings at a fixed horizontal spacing of about 280 km. The number of soundings required to cover the target regions is 10, 40, 160 and 640. Figure 2 shows the sounding locations in targets S, M and L. The fractional reduction of forecast error variance is plotted in Fig. 3a. As the sampled area and the number of soundings are increased the forecast error variance decreases. The reduction of forecast error variance is approximately proportional to the logarithm of the number of soundings up to about 160 soundings. This corresponds to a target region size of $13 \times 10^6\,\text{km}^2$. Further enlarging the target region beyond this size yields only a moderate additional reduction of forecast error variance.

As the goal is to find a set of supplementary observations to reduce the magnitude of the error projected in the subspace spanned by the leading routine Hessian singular vectors, targets based on these singular vectors should be superior to other targets. To demonstrate this, the experiment with 40 soundings is repeated with a medium size target region computed from total energy singular vectors. As anticipated, the forecast error variance is reduced significantly less with the observations in the total energy singular vector target than with
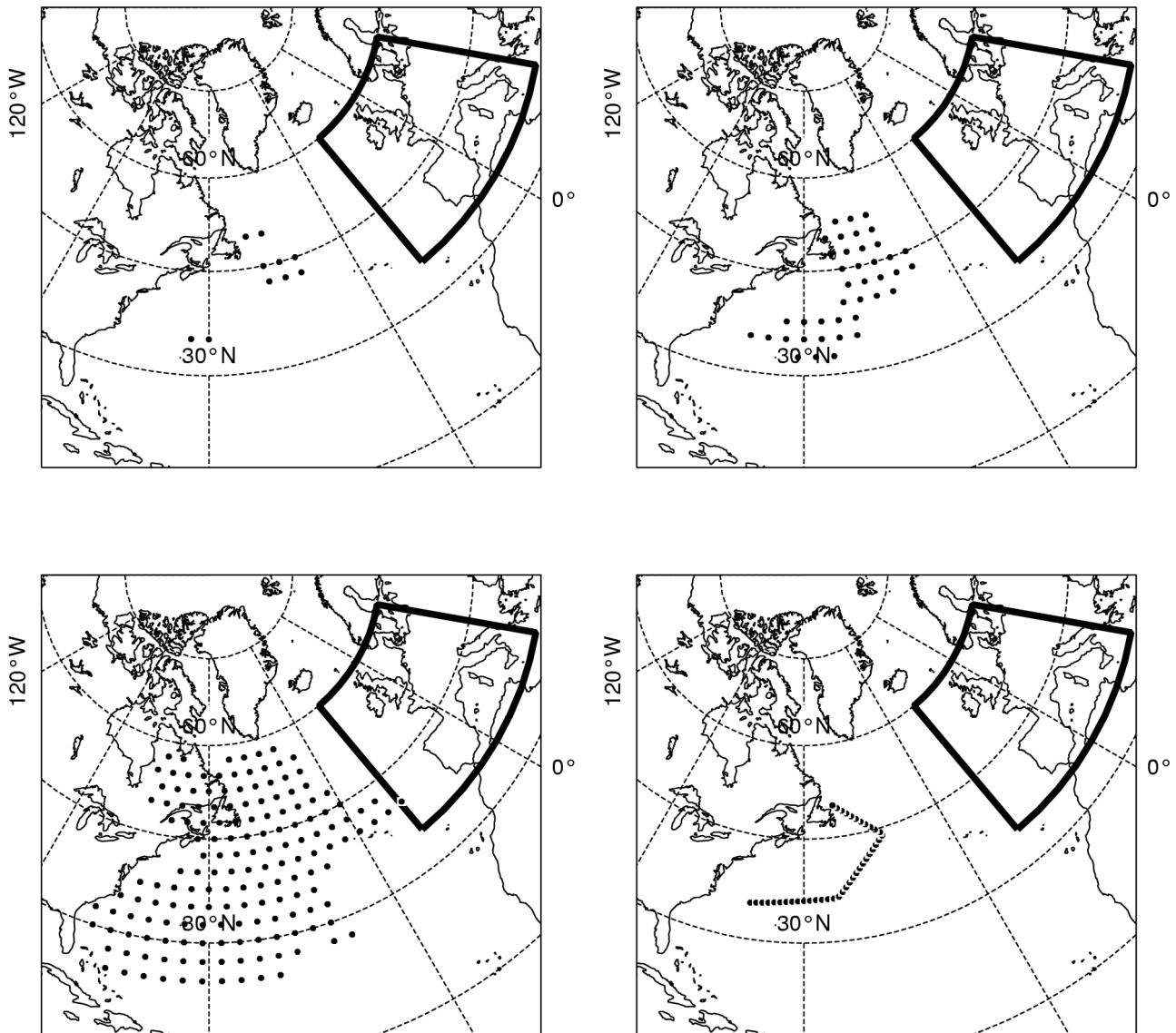
Figure 2: Sounding locations at 280 km spacing in targets S, M, L and along a hypothetical flight-track through target M. Number of soundings: 10, 40, 160 and 40. The box indicates the verification region.

observations in target M, which is based on Hessian singular vectors (Fig. 3a).

In a scenario with a fixed number of supplementary soundings, the HRR estimate can be used to determine the optimal horizontal spacing between soundings. As example the deployment of 40 targeted soundings is considered. The spacing is varied between 111 km and 1110 km. The target regions are computed again from the routine Hessian singular vectors. The area of the target regions is approximately 40 times the square of the spacing. The 280 km spacing yields the largest reduction of forecast error variance (Fig. 3b). One would expect that the optimal spacing has the same order of magnitude as the horizontal correlation length scale of the background error estimate used in the assimilation scheme (Leutbecher *et al.* 2002). The result is consistent with this expectation as the average horizontal correlation length scales of the background errors for surface pressure, vorticity, the unbalanced parts of divergence and temperature are about 400, 200, 200, and 300 km, respectively.
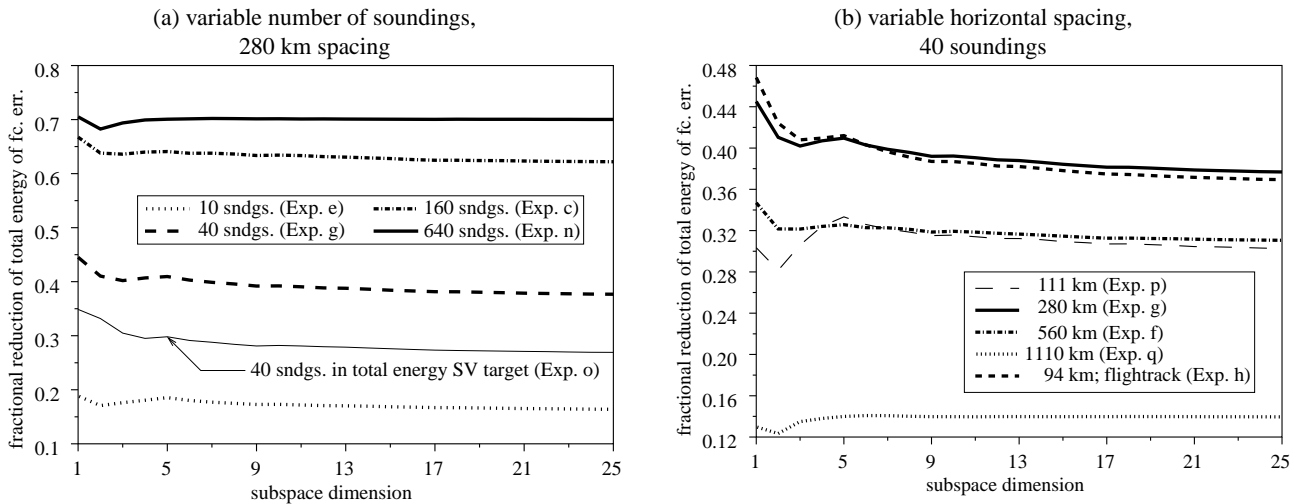
Figure 3: Fractional reduction of the total energy of forecast error r_n/ε_n versus subspace dimension n for network upgrades that differ in terms of spatial coverage.

With the optimal spacing of 280 km, target M is sampled homogeneously. However, the two-dimensional sampling pattern is not feasible if the soundings were to be obtained with sondes dropped from one aircraft. Figure 2 shows a rearrangement of the 40 sondes along a hypothetical flight-track in target M. As in the previous experiments, all soundings are simultaneous observations. Intuitively, one would expect that the one-dimensional pattern along the chosen flight-track is less suited to constrain the initial condition error in target M than the two-dimensional pattern. Yet, the reductions of forecast error variance due to the two patterns are almost identical up to a subspace dimension of 25 (Fig. 3b). Without rank reduction, the two patterns could nevertheless yield different reductions of forecast error variance. However, it may require a subspace dimension considerably higher than 25 to let this different performance emerge.

The flight-track had been chosen such that it traverses the entire target M but is not too long at the same time. It is 3700 km long with a sounding every 94 km. Obviously, the choice of the flight-track within target M matters. One could design another flight-track of about the same length in target S, which is contained in target M, to get the two-dimensional sampling with 111 km spacing between sondes. According to the HRR predictions, the sondes dropped along the latter flight-track yield a significantly smaller reduction of forecast error variance than the sondes along the former flight-track.

All experiments discussed so far study the horizontal distribution of observations. Every sounding extends from the surface to 200 hPa. One experiment has been repeated using only data either below 600 hPa or above 600 hPa to compare the impact of data from the lower troposphere with that from the upper troposphere. The sounding locations are the same as in experiment g, which has 40 soundings in target M at a spacing of 280 km. The experiment which uses the lower (upper) tropospheric part of the soundings yields 67% (56%) of the reduction of forecast error variance obtained with the entire sounding for a subspace dimension 25. Thus, the data in the lower troposphere reduce the forecast error variance somewhat more than the data in the upper troposphere. This may appear perplexing at first because the average total energy of Hessian singular vectors above 600 hPa is almost double the total energy below 600 hPa. However, the appropriate metric to assess the impact of the supplementary observations is the observation error covariance metric $\mathbf{H}_s^{\mathrm{T}}\mathbf{R}_s^{-1}\mathbf{H}_s$, cf. (29). This metric varies with altitude. For radiosonde data, the observation error variance for wind at 300 hPa is 2.6 times as large as the corresponding variance at 850 hPa. As a result of this weighting, the Hessian singular vectors contribute to the $\mathbf{H}_s^{\mathrm{T}}\mathbf{R}_s^{-1}\mathbf{H}_s$ metric about equal amounts above 600 hPa and below 600 hPa.

3.2   Observation type

The adaptation of the observing network to specific forecast goals could involve more than the choice of a spatial pattern for a set of additional observations. Upgrades of the observing network that differ in terms of the observed variables can be compared with the HRR estimate. To illustrate, the experiment with 40 soundings in target M at 280 km spacing is repeated twice using either wind data only or temperature data only. The reduction of forecast error variance due to wind observations is significantly larger than the reduction due to temperature observations (Fig. 4a). It has to be anticipated that these results are sensitive to the formulation of the balance between wind and mass in the statistical model for the background error covariances. The reduction obtained with soundings of wind and temperature is 20% smaller than the sum of the individual reductions. This is to be expected as wind and temperature increments are statistically balanced via the background error covariances. Thus, the two variables do not provide completely independent information.
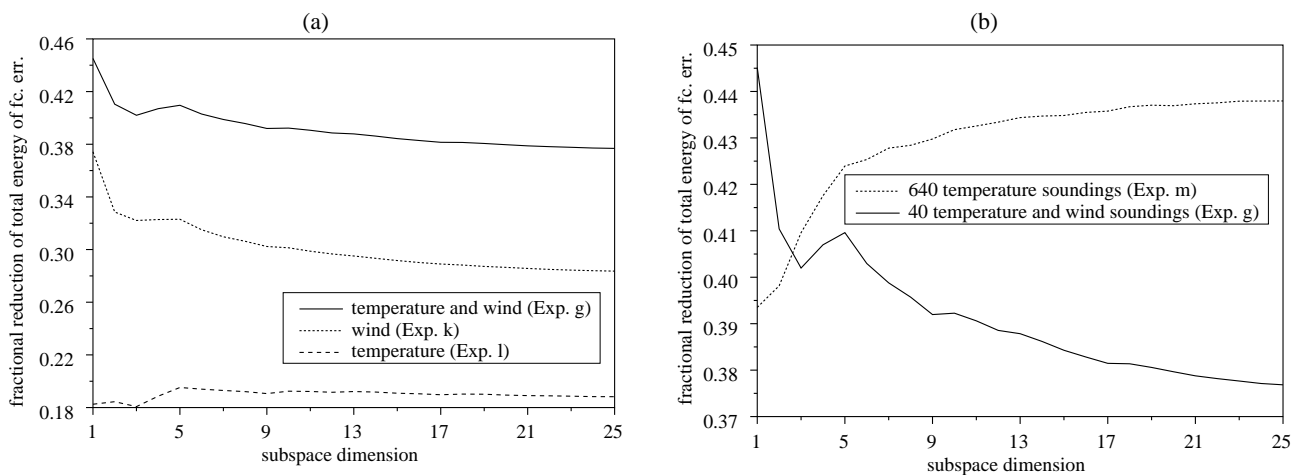

Figure 4:   Fractional reduction of the total energy of forecast error r_n/ε_n versus subspace dimension n for network upgrades that differ in terms of observation type.

More complex comparisons could be envisaged. Say, one had the following two options of complementing the routine observations: (i) a satellite that was able to provide 640 temperature soundings in target XL with the accuracy and the vertical resolution of *in situ* temperature measurements taken by a radiosonde or (ii) 40 dropsondes in target M that deliver temperature and wind data. The expected reductions of the total energy of forecast error for the two options are plotted in Fig. 4b. The dependence of the reduction of forecast error variance on the subspace dimension is interesting. The 40 soundings of wind and temperature observations are superior for a subspace of dimension one or two. However, for a subspace dimension greater three, the "satellite data" are the superior choice. Obviously, more complexity could be added to make the comparison more realistic, e.g. radiance observations in cloud-free regions could be compared with a set of *in situ* observations of wind and temperature. The impact of using more accurate instruments on future satellites can be assessed also if observation operators and realistic observation error estimates are available.

4   Discussion

An important question is whether the HRR estimate provides useful predictions of the change of forecast error variance due to modifications of the observing network. For the studied cyclone of 26 December 1999 the predictions of the HRR for some network upgrades can be compared with actual reductions of the total

Exp.	HRR	RUO	$\overline{\text{RPO}}$
d	0.16	0.11	0.11
e	0.16	0.09	–
o	0.27	0.31	0.25
f	0.31	0.32	–
g	0.38	0.35	0.20
c	0.62	0.52	–

HRR: expected fractional reduction in the 25-dim subspace

RUO: realized fractional reduction with unperturbed observations

$\overline{\text{RPO}}$: realized fractional reduction with perturbed observations, average over five realizations of observational error

Table 2: Hessian reduced rank predictions versus realized fractional reductions of the total energy of the full forecast error as determined in OSSEs.

energy of the 48-hour forecast error in the verification region as obtained in the corresponding observing system simulation experiments (OSSEs) of Leutbecher *et al.* (2002). Note, that in some of the experiments a small fraction of sounding locations disagrees between the HRR experiments and the OSSEs because the target regions are diagnosed in a slightly different manner. In Table 2 the fractional reductions of the total energy of the full forecast error $(\|\mathbf{Px}_{\text{cnt}}\|_E^2 - \|\mathbf{Px}\|_E^2)/\|\mathbf{Px}_{\text{cnt}}\|_E^2$ are listed for the OSSEs, where $\mathbf{x}$ denotes the state vector of the forecast error of the experiment with the supplementary observations and $\mathbf{x}_{\text{cnt}}$ the state vector of the forecast error of the control experiment, which uses no supplementary observations. The magnitude of the HRR predictions of the fractional reduction agrees surprisingly well with actual realizations. However, this agreement may be mere coincidence as results for a single realization of the error of the control experiment are compared with expected values for distributions of initial errors.

A thorough multi-case evaluation consisting of two steps could be envisaged. First, the HRR estimate is compared with the actual forecast error projected into the subspace of leading Hessian singular vectors. Second, the projected forecast error is compared with the total forecast error. The test will require many assimilation experiments with a modified observing network in order to obtain a reliable estimate of the mean of the actual change of the square norm of forecast error. One could study the expected reduction of forecast error variance due to the addition of targeted dropsondes during the recent field campaigns FASTEX, NORPEX and the WS-RPs similar to the work of Majumdar *et al.* (2001) for the ETKF. Another option to test the HRR estimate is to suppress data from the routine observing network and quantify the associated increase of forecast error variance. In these data denial experiments, one would not be restricted to the limited number of cases in recent field campaigns.

The climatological background error covariances used for the HRR estimate correspond to a certain routine observing network. This implies that the HRR estimate is a tool to investigate intermittent changes of this routine observing network. Any permanent change of the routine network would affect the climatological background error. Therefore, the assimilation experiments should not be cycled in the evaluation proposed above. The reliance on the climatological background error covariances employed in the variational assimilation scheme is probably the largest weakness of the HRR. Further improvements of it will have to aim for better background error estimates, which should account for past changes of the observing network and the actual atmospheric flow.

Inaccuracies in the observation error estimates may be another cause for discrepancies between the HRR predictions and the actual reduction of forecast error variance. Correlations of observation error are usually neglected in current operational assimilation schemes. For instance, satellite radiance data will have observation errors correlated in space and between different spectral channels. The HRR estimate may overestimate the impact of such data if the correlations are not accounted for. Furthermore, model error may contaminate the relation between the HRR predictions and the actual square norm of forecast errors. This includes errors of the nonlinear forecast model itself as well as errors of the tangent-linear version of the forecast model. Another issue that may be of relevance in the proposed evaluation is the consistency between the HRR estimate and the assimilation system. Ideally, the spatial resolution of the analysis increments should agree with the resolution used in the HRR. In addition, the data selection choices made for the assimilation should agree with the data selection choices used in the computation of the Hessian metric. There is a further consistency issue for implementations of incremental 4D-Var that recompute the trajectory used for the linearization during the minimization of the quadratic cost function. This update of the trajectory is not accounted for in the estimate of the analysis error covariances used in the HRR.

Two alternative approximations were proposed to calculate the variance of the projected forecast error. The analysis error covariances are approximated at different stages in the two methods. In the first method (sections 2b-d), the metrics $\mathbf{A}^{-1}$ and $\widetilde{\mathbf{A}}^{-1}$ are fully consistent with the covariance estimates used in the assimilation scheme. The approximation occurs when the projected analysis error covariance matrix for the modified network is represented by the outer product of the subspace singular vectors. The second method (section 2f), starts with an approximation of the analysis error covariance matrix for the routine observing network. The covariance matrix is represented by the background error covariance matrix of the assimilation scheme plus a low rank correction that describes the leading effect of the observations on the covariance matrix. Thereafter no further approximation is required. It remains to be investigated which of these approximation techniques is better suited for the computation of the reduction of forecast error variance.

So far in this paper changes of the variance of forecast error projected into a fixed subspace were studied. The subspace is spanned by the singular vectors computed with the Hessian of the routine observing network. However, the subspace that evolves into the leading eigenvectors of the forecast error covariance matrix will change as the observing network is modified. The HRR estimate using a fixed subspace will not provide a method to determine the optimal sampling strategy for a set of supplementary observations, if the subspace changes significantly due to the addition of these extra observations in the Hessian metric. To address this issue, Hessian singular vectors were computed for the modified networks of experiments f and g with 40 supplementary soundings at 560 km spacing and 280 km spacing, respectively. The agreement between the subspaces spanned by these modified Hessian singular vectors and the routine Hessian singular vectors is quantified with a similarity index which is 1 for identical subspaces and 0 for completely orthogonal subspaces (Buizza 1994). The index is computed with the total energy metric using orthonormalized bases with respect to this metric. For a subspace dimension of 25, the similarity indices are 0.86 for experiment f (560 km spacing) and 0.82 for experiment g (280 km spacing). Thus, the subspaces are still fairly similar if 40 targeted soundings are added to the routine observing network. Therefore, it appears justified to optimize observing network upgrades of this extent using a fixed subspace.

The illustration of the HRR in a case study was performed in a diagnostic mode. In order to apply the technique in real-time for planning adaptive observations Hessian singular vectors need to be computed at a lead time of 24–48 h with respect to the network modification time. This requires a prediction of the likely distribution of observations and the use of a trajectory starting from a forecast. Buizza and Montani (1999) and Gelaro *et al.* (1999) investigated the sensitivity of total energy singular vectors to the forecast lead time of the used trajectory. They found significant differences between singular vector subspaces computed with 0 h lead and with 48 h lead mostly due to differences in structure rather than location. It is conceivable that Hessian singular

vector subspaces are also sensitive to the trajectory lead time. Therefore, it is important to check in subsequent work that the HRR predictions of the reduction of forecast error variance are reasonably insensitive to the lead time. Apart from the choice of trajectory, an additional sensitivity is expected for the Hessian singular vectors due to inaccuracies in predicting the spatial distribution of observations. For instance, the spatial distribution of satellite observations that depend on the location of clouds will be difficult to predict accurately.

It may be justified to simplify the initial time metric for the routine observing network given the potential difficulties in predicting the variable parts of the observing network accurately enough and given the approximations made in current variational schemes of modelling the background error covariance by a climatological estimate. One attempt could be to replace the routine Hessian by a metric based on a climatological estimate of the analysis error covariances. The covariances could be parameterized in the same way as the background error covariances. The parameters for the climatological analysis error covariance could be estimated from an ensemble of analyses generated with different random perturbations of the observed values for each ensemble member. Such an ensemble is used to determine the operational background error covariances at ECMWF (Fisher and Andersson 2001). A further advantage of this simplification would be the reduced computational cost for obtaining the singular vector subspace. The computational cost of calculating singular vectors with the climatological analysis error covariance metric will be roughly comparable to the cost of calculating total energy singular vectors as the Lanczos algorithm can be used in both cases. The Hessian singular vectors are substantially more expensive to compute as a generalized eigenproblem solver is required that evaluates the gradient of the cost function many times for each iteration step. The high computational cost together with lacking evidence of a benefit for the ensemble prediction system has precluded the operational use of Hessian singular vectors so far.

5   Conclusions

A new tool for adaptive observations has been introduced: The Hessian reduced rank estimate (HRR) predicts how much the expected value of the square norm of forecast error changes due to an intermittent modification of the observing network. The HRR estimate is based on a variational assimilation scheme using the incremental approach. Forecast errors are projected into the subspace spanned by the leading Hessian singular vectors computed for the routine observing network. Forecast errors are quantified with a norm such as total energy. The expected value of the square of this norm is computed for distributions of initial error that are consistent with the statistical assumptions of the variational assimilation scheme. In the one-dimensional case, forecast errors are projected on the leading Hessian singular vector. This rank-one version of the HRR estimate is closely linked to the Kalman filter sensitivity (Bergot and Doerenbecher 2002). If the HRR estimate is applied to the full state space, it yields the same predictions as an extended Kalman filter — provided that the Kalman filter is initialized with the background error covariance matrix used in the variational assimilation scheme.

A potential advantage of the HRR is its consistency with an operational assimilation scheme. The ensemble transform Kalman filter (ETKF) technique applied to a set of evolved ensemble perturbations lacks this consistency. However, if the ETKF technique is applied to a set of Hessian singular vectors it predicts the same reductions of forecast error variance as the HRR — provided the same measure of forecast error, the same observation operator and the same observation error covariances are used. Thus, practically both techniques can be made to agree. The different way of deriving the two techniques may be of educational interest. In the derivation of the ETKF, the reduction of rank is introduced by assuming that the full prediction error covariance matrix is represented by an outer product of transformed ensemble perturbations. Therefore, the terms in $\mathbf{F}$ in (19) are implicitly assumed to vanish and the issue addressed in appendix B does not emerge. The rank reduction remains implicit through the choice of the ensemble size. For the HRR, the rank reduction via a projection operator is explicit throughout the derivation. The latter approach is attractive as it offers different options of

approximating the projected versions of the analysis error covariance matrices.

Several aspects of the adaptive observation problem were studied with the HRR estimate in a case study for an extra-tropical storm. The relation between the size of the adaptive component of the observing network and the expected reduction of the total energy of the forecast error was determined. For a given number of targeted soundings distributed in a two-dimensional pattern, the optimal horizontal spacing between soundings was determined. The optimal value coincides with the average horizontal correlation length scale of the background error estimate. The reduction of forecast error variance due to data from the lower troposphere was compared with that due to data from the upper troposphere. Furthermore, the impact resulting from observations of different variables was determined.

Acknowledgements

Appendix A: Projections

Now, the equivalence (7) of projecting at initial time on L_n or at final time on $\mathbf{PM}L_n$ is proved. Using the singular value decomposition (2), the orthonormality relations (3), (4) and the definition of the projections (5),(6) we observe that

$$\mathbf{PM\Pi}_n = \mathbf{U\Sigma V}^\mathrm{T}\mathbf{A}^{-1}\mathbf{V}_n\mathbf{V}_n^\mathrm{T}\mathbf{A}^{-1} = \mathbf{U\Sigma}\begin{pmatrix}\mathbf{I}_n & \mathbf{0}\\ \mathbf{0} & \mathbf{0}\end{pmatrix}\mathbf{V}^\mathrm{T}\mathbf{A}^{-1} = \mathbf{U}\begin{pmatrix}\mathbf{I}_n & \mathbf{0}\\ \mathbf{0} & \mathbf{0}\end{pmatrix}\mathbf{\Sigma V}^\mathrm{T}\mathbf{A}^{-1} =$$

$$\mathbf{U}_n\left(\mathbf{I}_n\ \mathbf{0}\right)\mathbf{\Sigma V}^\mathrm{T}\mathbf{A}^{-1} = \mathbf{U}_n\mathbf{U}_n^\mathrm{T}\mathbf{EU\Sigma V}^\mathrm{T}\mathbf{A}^{-1} = \widehat{\mathbf{\Pi}}_n\mathbf{PM}. \quad \text{(A1)}$$

Appendix B: Approximation of the projected covariance matrix

For the modified observing network, the analysis error covariance matrix projected onto the subspace L_n has been approximated by (22). The approximation of the projected covariance matrix can be improved, if the modified metric is known in a larger subspace $L_{n'}$, $n' > n$. Now, it is investigated how the approximation of the covariance matrix affects the value of the forecast error variance.

The exact projected covariance matrix is given by (21). It involves the matrix $\mathbf{F} = \widetilde{\mathbf{V}}_n^\mathrm{T}\widetilde{\mathbf{A}}^{-1}(\tilde{\mathbf{v}}_{n+1}\ldots\tilde{\mathbf{v}}_N)$, which can be split as $\mathbf{F} = (\mathbf{F}'\ \mathbf{F}'')$ with

$$\mathbf{F}' \equiv \widetilde{\mathbf{V}}_n^\mathrm{T}\widetilde{\mathbf{A}}^{-1}(\tilde{\mathbf{v}}_{n+1}\ldots\tilde{\mathbf{v}}_{n'}) \quad \text{and} \tag{A2}$$

$$\mathbf{F}'' \equiv \widetilde{\mathbf{V}}_n^\mathrm{T}\widetilde{\mathbf{A}}^{-1}(\tilde{\mathbf{v}}_{n'+1}\ldots\tilde{\mathbf{v}}_N). \tag{A3}$$

An improved approximation of the projected covariance matrix $\mathbf{\Pi}\widetilde{\mathbf{A}}\mathbf{\Pi}^{\mathrm{T}}$ is obtained by replacing $\mathbf{F}$ with $(\mathbf{F}'\ \mathbf{0})$ in (21). With this new approximation, the forecast error variance becomes

$$\tilde{\varepsilon}_n \approx \mathrm{tr}\left(\left(\mathbf{I}_n - \mathbf{F}'\mathbf{F}'^{\mathrm{T}}\right)^{-1}\widetilde{\mathbf{\Lambda}}\right). \tag{A4}$$

To compute $\mathbf{F}'$, an $\widetilde{\mathbf{A}}^{-1}$-orthonormal basis $\widetilde{\mathbf{V}}' \equiv (\tilde{\mathbf{v}}_{n+1}\ldots\tilde{\mathbf{v}}_{n'})$ of $\mathrm{span}\{\mathbf{v}_{n+1},\ldots,\mathbf{v}_{n'}\}$ is required. Define $\mathbf{V}' \equiv (\mathbf{v}_{n+1}\ldots\mathbf{v}_{n'})$ and $\mathbf{C}'' \equiv \mathbf{V}'^{\mathrm{T}}\widetilde{\mathbf{A}}^{-1}\mathbf{V}'$. Then, the new basis is obtained via the transformation $\widetilde{\mathbf{V}}' = \mathbf{V}'\mathbf{\Gamma}'$, where the transformation matrix $\mathbf{\Gamma}'$ satisfies

$$\mathbf{\Gamma}'^{\mathrm{T}}\mathbf{C}''\mathbf{\Gamma}' = \mathbf{I}_{n'-n}. \tag{A5}$$

With this transformation, $\mathbf{F}'$ is given by

$$\mathbf{F}' = \mathbf{\Gamma}^{\mathrm{T}}\mathbf{C}'\mathbf{\Gamma}', \tag{A6}$$

with $\mathbf{C}' \equiv \mathbf{V}_n^{\mathrm{T}}\widetilde{\mathbf{A}}^{-1}\mathbf{V}'$.

Fig. B1 shows the improved approximation (A4) versus the original approximation (23) for cases where the routine observations where supplemented with 10–640 soundings in targets S, M, L and XL. The experiments with the larger number of soundings represent a major change of the observing network in the region of interest. The expected total energy of the forecast error appears to converge rapidly as the dimension n' is increased. The difference between the two approximations is largest for the lowest dimensional subspaces ($n < 5$). For the subspaces with dimension 5–10, the total energy of forecast error computed with the original approximation has reached already 95% of the value computed with the improved approximation for $n' = 25$. This suggests that the original approximation is good enough if the subspace dimension n is sufficiently large, say greater than five.
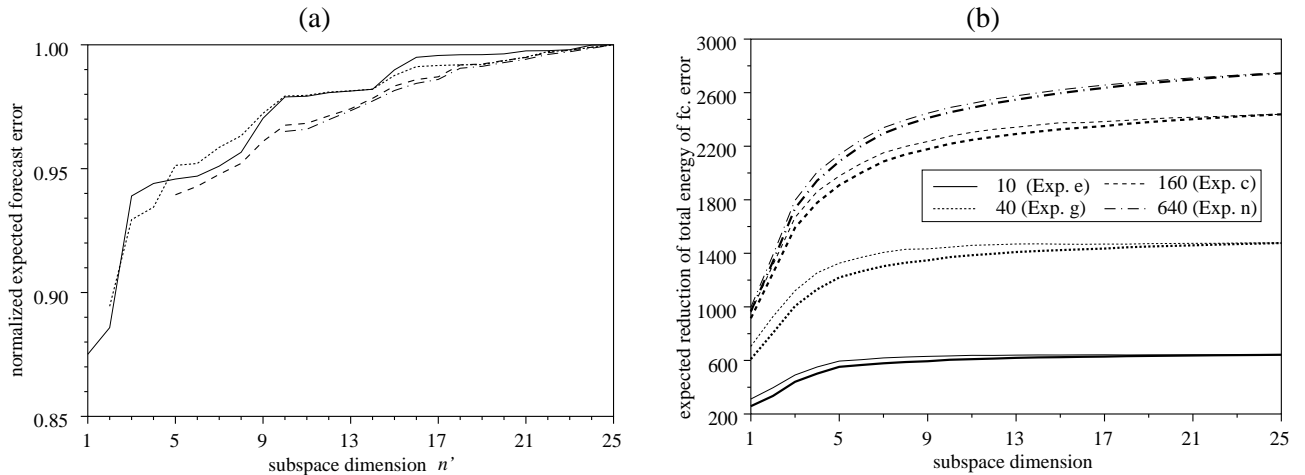

Figure B1: Impact of improving the approximation of the projected covariance matrix $\mathbf{\Pi}_n\widetilde{\mathbf{A}}\mathbf{\Pi}_n^{\mathrm{T}}$. (a) Convergence of the expected total energy of forecast error projected on the 1, 2, 5 and 10-dimensional subspaces versus the dimension n' of the subspace used to approximate the projected covariance matrix. Experiment g with 40 soundings in target M. The total energy of the forecast error is normalized with the value obtained for $n' = 25$. (b) The expected reduction of forecast error variance versus the subspace dimension n using the original approximation of the covariance matrix ($n' = n$, normal) and the improved approximation ($n' = 25$, bold). Experiments with 10, 40, 160 and 640 soundings in targets S, M, L and XL, respectively.

References

Baker, N. L. and R. Daley, 2000: Observation and background adjoint sensitivity in the adaptive observation-targeting problem. *Quart. J. Roy. Meteor. Soc.*, **126**, 1431–1454.

Barkmeijer, J., M. Van Gijzen, and F. Bouttier, 1998: Singular vectors and estimates of the analysis-error covariance metric. *Quart. J. Roy. Meteor. Soc.*, **124**, 1695–1713.

Bergot, T. and A. Doerenbecher, 2002: A study on the optimization of the deployment of targeted observations using adjoint-based methods. *Quart. J. Roy. Meteor. Soc.*, **128**, 1689–1712.

Berliner, L. M., Z.-Q. Lu, and C. Snyder, 1999: Statistical design for adaptive weather observations. *J. Atmos. Sci.*, **56**, 2536–2552.

Bishop, C. H., B. J. Etherton, and S. J. Majumdar, 2001: Adaptive sampling with the ensemble transform Kalman filter. Part I: Theoretical aspects. *Mon. Wea. Rev.*, **129**, 420–436.

Bishop, C. H. and Z. Toth, 1999: Ensemble transformation and adaptive observations. *J. Atmos. Sci.*, **56**, 1748–1765.

Buizza, R., 1994: Localization of optimal perturbations using a projection operator. *Quart. J. Roy. Meteor. Soc.*, **120**, 1647–1681.

Buizza, R. and A. Montani, 1999: Targeting observations using singular vectors. *J. Atmos. Sci.*, **56**, 2965–2985.

Doerenbecher, A. and T. Bergot, 2001: Sensitivity to observations applied to FASTEX cases. *Nonlinear Processes in Geophysics*, **8**, 467–481.

Fisher, M. and E. Andersson, 2001: Developments in 4D-Var and Kalman filtering. Technical report, ECMWF Tech. Memo 347.

Fisher, M. and P. Courtier, 1995: Estimating the covariance matrices of analysis and forecast error in variational data assimilation. Technical report, ECMWF Tech. Memo **220**.

Gelaro, R., R. H. Langland, G. D. Rohaly, and T. E. Rosmond, 1999: An assessment of the singular-vector approach to targeted observing using the FASTEX data set. *Quart. J. Roy. Meteor. Soc.*, **125**, 3299–3327.

Leutbecher, M., J. Barkmeijer, T. N. Palmer, and A. J. Thorpe, 2002: Potential improvement to forecasts of two severe storms using targeted observations. *Quart. J. Roy. Meteor. Soc.*, **128**, 1641–1670.

Majumdar, S. J., C. H. Bishop, B. J. Etherton, I. Szunyogh, and Z. Toth, 2001: Can an Ensemble Transform Kalman Filter predict the reduction in forecast error variance produced by targeted observations? *Quart. J. Roy. Meteor. Soc.*, **127**, 2803–2820.

Palmer, T. N., R. Gelaro, J. Barkmeijer, and R. Buizza, 1998: Singular vectors, metrics, and adaptive observations. *J. Atmos. Sci.*, **55**, 633–653.

Rabier, F. and P. Courtier, 1992: Four-dimensional assimilation in the presence of baroclinic instability. *Quart. J. Roy. Meteor. Soc.*, **118**, 649–672.